

**THERMOMECHANICAL PROCESSING AND CONTINUOUS COOLING
TRANSFORMATION BEHAVIOR OF IN-718**

C.I. Garcia, A.K. Lis, E.A. Loria* and A.J. DeArdo

**Basic Metals Processing Research Institute
Department of Materials Science and Engineering
Materials Research Center
University of Pittsburgh**

***Niobium Products Company, Inc.**

ABSTRACT

The influence of homogenization treatment and cooling rates on the transformation characteristics of IN-718 alloy were studied. In addition, the effect of thermomechanical processing on the recrystallization behavior of this alloy was also investigated. The results of this investigation led to both the construction of continuous cooling transformation diagrams and to the establishment of a temperature-deformation-recrystallization map for this alloy.

INTRODUCTION

During the last decade, important advances in melting and casting technologies have resulted in significant improvements in the homogeneity and microstructural control of as-cast IN-718 alloys.⁽¹⁻⁴⁾ However, these advances have not been matched with an equal understanding in the science and technology of microstructural control during the hot deformation of these alloys (i.e. forging of large ingots). For example, the typical commercial processing of IN-718 alloys leads to a very heterogeneous grain structure which is carried through the final forging and heat treatments. This heterogeneous structure decreases the performance of the final components.⁽⁵⁾ The ability to control the microstructure (i.e. refinement) during the ingot-to-billet conversion process requires a fundamental understanding of the way in which IN-718 alloys respond to thermomechanical processing (TMP) and how that response can be altered. Since, the central goal of TMP is the control of the high temperature grain structure, the knowledge of the overall microstructure prior to TMP is essential. Of particular interest is the understanding of the way in which a given homogenization treatment and cooling rate influences the transformation characteristics of IN-718 alloys. Several workers have investigated the effect of homogenization treatments on the transformation characteristics of alloy 718 on heating.⁽⁶⁻¹³⁾ These studies defined the temperatures at which a given phase transformation takes place. Other studies, have analyzed the kinetics of precipitation reactions in 718 and other similar alloys under isothermal conditions.⁽¹⁴⁻¹⁷⁾ These investigations have established the processing conditions for enhanced precipitation response during the final heat treatment (i.e. aging) of IN-718 alloys. However, despite the large amount of microstructural information published in the literature very few studies have attempted to map the microstructural condition of IN-718 alloys prior to TMP.^(18,19) That is, the microstructure which results after a given homogenization treatment and continuously cooled to the deformation temperature prior to the ingot-to-billet conversion process. It is well-known that isothermal transformation diagrams are very useful in defining heat treatments and in understanding why a given material responds as it does to a particular heat treatment. However, these diagrams cannot be used to predict precisely the path of transformation as it takes place during continuous cooling conditions. Therefore, the literature on the metallurgical state of IN-718 alloy prior to cogging practice is limited.⁽⁵⁾

The major goal of this paper was to study the effect of various homogenization treatments and cooling rates on the transformation characteristics of IN-718 alloy. A second objective of this study was to define a temperature-deformation-recrystallization map for this alloy. The results of this investigation will be presented and discussed.

EXPERIMENTAL PROCEDURE

The samples used in this study were sectioned from the top, middle and bottom of a 530 mm. diameter VAR ingot of Alloy 718. The chemical composition in wt% of the ingot as well as the overall sample sectioning are shown in Figure 1.

DILATOMETRY

The effect of the prior homogenization treatment and cooling rate on the transformations characteristics of IN-718 alloy were conducted in a modified Theta Dilatronic V system. This system has been modified to obtain cooling rates from 100°C/s to 0.001°C/s. Three homogenization treatments under vacuum conditions prior to the dilatometry studies were used. For example, one set of samples was homogenized at 1180°C for 24 hrs, the second set of samples for 72 hrs and the third set for 90 hrs at the same temperature. Samples from these conditions were machined to a size of 30.0 mm. long x 3.0 mm. diameter. These samples were then used for the dilatometry studies. The results from these experiments led to the construction of the continuous cooling transformation (CCT) diagrams.

HOT DEFORMATION STUDIES

The establishment of the temperature-deformation-recrystallization map for the IN-718 alloy was performed using a computer-controlled MTS machine dedicated to high temperature deformation studies. The details of the sample preparation, machine capabilities and processing parameters for this alloy have been discussed in previous publication.⁽¹⁹⁾

MICROSTRUCTURE

The samples for optical microscopy examination were prepared using standard metallographic techniques. The etching solution used to reveal the

microstructure consisted of: 50 ml H₂O (distilled) + 40 ml HCl + 10 ml HF + 2-3 ml H₂O₂. The samples were immersed in the solution for 10 to 40 seconds. Samples for scanning electron microscopy (SEM) and transmission electron microscopy (TEM) observation were prepared using standard sample preparation techniques. These samples were examined in transmission using a JOEL 200CX electron microscope operated at 200 KV. The SEM examination was conducted in a JOEL JSM-35CF scanning electron microscope.

RESULTS AND DISCUSSION

CONTINUOUS COOLING TRANSFORMATION (CCT) DIAGRAMS

It is well understood that the final microstructure, and hence, the mechanical properties of a given alloy system, are dependent upon: a) the metallurgical condition of the parent phase (i.e. high temperature phase) prior to transformation, and b) the transformation behavior of the parent phase at a given cooling condition. Therefore, the knowledge of the as-reheated microstructure and subsequent transformation characteristics after cooling in terms of the constituents present (e.g. grain size, type of precipitates, etc.) is of primary importance to devise appropriate TMP schemes to achieve the required microstructural refinement. In the present study, the fundamental understanding of the γ microstructure prior to and after TMP is essential, since, the microstructural response of the γ grain size during TMP will be strongly influenced by forces which may act to enhance or retard its recrystallization behavior. One of the methods available to establish the precise microstructural evolution from a given starting and cooling conditions is through the construction of CCT diagrams.

The CCT diagrams developed for IN-718 as function of homogenization treatment are shown in Figures 2, 3 and 4. A comparison of the results from these diagrams indicate a shift to longer times in the transformation reactions with increasing homogenization time. In addition, the results from the CCT diagram after the 90 hrs homogenization treatment appears to indicate two major differences when compared to the CCT diagrams after the 24 and 72 hrs homogenization treatments. For example, the first difference is the shift in the δ -phase transformation start temperature to lower temperatures. The δ -phase transformation temperature is depressed by about 120°C. The second difference is that the nucleation of new and small MC-type of carbides precedes the formation of the δ -phase. A possible explanation of this behavior could be based on the fact that at the homogenization temperature used in this study, 1180°C, and the long holding times, the combined dissolution of Laves phase, small primary MC-type of carbides and other Nb-rich phases increases the supersaturation on Nb in the matrix and also reduces the chemical segregation of Nb at γ grain boundaries. By reducing the local concentration of Nb at grain boundaries the formation of δ -phase is suppressed for relatively fast cooling rates. Hence, on cooling from the homogenization temperature the Nb supersaturation of the matrix increases and the precipitation of MC-type carbides is favored over that of δ . Similar type of fine precipitation of MC-type carbides has been reported elsewhere.⁽²¹⁻²³⁾ These MC-type carbides are NbC which later decompose to generate more γ'' in the alloy upon further cooling.⁽²²⁾

TEMPERATURE-RECRYSTALLIZATION-TIME MAP

The temperature-recrystallization-time map for IN-718 alloy determined at a $\epsilon=0.2$ and $\epsilon=0.5s^{-1}$ is presented in Figure 5. This figure describes the recrystallization behavior of this alloy under dynamic and static conditions. The samples used in this part of the study were homogenized at 1180°C for 24 hrs. The time coordinates represent the holding time at deformation temperature prior to quenching. The results shown in this figure indicate a series of points: (1) at deformations equal to or less than $\epsilon=0.2$, full dynamic recrystallization can take place if the deformation process occurs at very high temperatures, that is above 2150°F (1177°C); (2) at lower temperatures, about 1960°F (1071°C) full recrystallization can be obtained under static conditions; (3) partial recrystallization is obtained between 1960 and 1780°F (1071 to 962°C); (4) below 1780°F the fully unrecrystallized zone is observed. The results presented in Figure 5 also defines the recrystallization-stop temperatures, $T_{100\%}$ and $T_{0\%}$ for IN-718 alloy under the TMP conditions used in this study.

MICROSTRUCTURE

Typical examples of TEM and SEM micrographs obtained after the various homogenization treatments and cooling rates used in the construction of the CCT diagrams are illustrated in Figures 6 through 10. Figure 6 shows the TEM microstructure after 24 hrs at 1180°C and cooled at 17°C/s. The TEM microstruc-

ture shows a highly dislocated structure and some stacking faults within the matrix. No evidence of MC-type precipitation or δ -phase was observed. At slower rates of cooling about 4°C/s and longer homogenization times δ -phase formation occurs, see Figure 7. This figure shows the formation of fine δ at primary γ grain boundaries. Figure 8 illustrates the co-existence of primary MC-type carbides, fine new MC precipitates and fine δ -phase. At very slow rates of cooling at about 1°C/min, the presence of Laves-phase, primary MC-type of carbides and the abundant precipitation of $\gamma'' + \gamma'$ precipitation was observed, Figure 9. A more detailed TEM micrograph of δ -phase, γ'' , and γ' precipitation is shown in Figure 10.

CONCLUSIONS

1. A pronounced effect on the transformation start temperatures of the phases which exist in Alloy 718 was observed with homogenization treatment. For example, the longer the homogenization treatment the lower the shift in transformation start temperature.
2. At short homogenization times δ -phase formation precedes the formation of new MC-type carbides. This is similar to formation of δ -phase from the as-cast condition.
3. At longer homogenization times the formation of δ -phase is suppressed. Precipitation of MC-type carbides takes place prior to δ -phase.
4. The formation of fine NbC was confirmed. These precipitates are not stable at very slow cooling rates. They decompose to aid in the formation of γ'' .
5. The understanding of the microstructural evolution (i.e. δ -phase and MC precipitation) prior to TMP can be used to control the recrystallization process of this alloy during the ingot-to-billet conversion process.

REFERENCES

1. L. W. Lherbier, "Melting and Refining", Superalloys II, ed. C.E. Sims (Wiley Interscience, New York 1987), 387-410.
2. A. Mitchell, Proc. Vac. Metallurgical Conference, AVS-I&SS (1986) 55-64.
3. M. D. Evans, Proc. Vac. Metallurgical Conference, AVS-I&SS (1986) 125-130.
4. J. T. Cordy et al., Proc. Vac. Metallurgical Conference, AVS-TMS (1984) 69-74.
5. E. A. Loria, "A Forward Look at Alloy 718" (Niobium Technical Report, NbTR-12/88, Niobium Products Company, Inc. Pittsburgh).
6. W. D. Cao et al., "Differential Thermal Analysis (DTA) Study of the Homogenization Process in Alloy 718", Proceedings of the International Symposium of Superalloys 718, 625 and Various Derivatives, E. A. Loria ed., (TMS-AIME Warrendale, PA 1991), 147-160.
7. A. S. Ballantyne and A. Mitchell, "The Prediction of Ingot Structure in VAR/ESR 718", in Sixth International Vacuum Metallurgy Conference Proceedings, ed. G. K. Bhat and R. Schattler, (San Diego, California, 1979), 599-627.
8. Yvonne C. Fayman, "Microstructural Characterization and Elemental Partitioning in a Direct-Aged Superalloy (DA718)", Materials Science & Engineering, 92 (1987), 159-171.
9. G. K. Bouse, "Application of a Modified Phase Diagram to the Production of Cast Alloy 718 Components", in Superalloy 718, Metallurgy and Applications, ed. E. A. Loria, (TMS, 1989), 69-77.
10. M. J. Cieslak, G. A. Knorovsky, T. J. Headley and A. D. Romig, Jr., "The Solidification Metallurgy of Alloy 718 and Other Nb-Containing Superalloys," Ibid 59-68.
11. M. J. Cieslak, T. J. Headley, G. A. Knorovsky, A. D. Romig, Jr. and T. Kollie, "A Comparison of the Solidification Behavior of INCOLOY 909 and INCONEL 718", Ibid, 21A (1990), 479-488.
12. G. A. Knorovsky, M. J. Cieslak, T. J. Headley, A. D. Romig, Jr. and W.F. Hammett, "Inconel 718. A Solidification Diagram", Metallurgical Transactions, 20A (1989), 2149-2158.

13. J. M. Poole, "Homogenization of VIM-VAR Inconel Alloy 718", in Conference Proceedings of the Special Melting and Processing Technologies, (San Diego, California, Moyes Publishers, 1988), 508-539.
14. W. J. Boesch and H. B. Canada, "Precipitation Reactions and Stability of Ni₃Cb in Inconel 718 Alloy", (Seven Springs International Symposium, 1968).
15. Basile and Radavich, "A Current T-T-T Diagram for Wrought Alloy 718", Proceedings of the International Symposium of Superalloys 718, 625 and Various Derivatives, E.A. Loria, ed., (TMS-AIME Warrendale, Pa., 1991), 147-160.
16. J.R. Caum, M.E. Adkins and W.G. Lipscomb, "Performance of High Nickel Alloys in Intermediate Temperature Refinery and Petrochemical Environments".
17. M. Kohler, "Effect of the Elevated-Temperature Precipitation in Alloy 625 on Properties and Microstructure, Superalloys 718, 625, and Other Derivatives", Proceedings of the International Symposium of Superalloys 718, 625, and Various Derivatives, E.A. Loria, ed., (TMS-AIME Warrendale, Pa., 1991), 147-160.
18. J. A. Corrado, W. H. Coutts and J. F. Radavich, TMS Paper No. A86-34, 1986).
19. C.I. Garcia, D.E. Camus, E.A. Loria and A.J. DeArdo, "Microstructural Refinement of As Cast Alloy 718 via Thermomechanical Processing", Proceedings of the International Symposium of Superalloys 718, 625, and Various Derivatives, E.A. Loria, ed., (TMS-AIME Warrendale, Pa., 1991), 147-160.
20. J.F. Radavich, "Metallography of Alloy 718", Journal of Metals, July, 1988.
21. M.G. Burke and M.K. Miller, "Precipitation in Alloy 718: a Combined AEM and APFIM Investigation", Proceedings of the International Symposium of Superalloys 718, 625, and Various Derivatives, E. A. Loria, ed., (TMS-AIME Warrendale, Pa., 1991), 147-160.
22. C. T. Sims, "A Perspective of Niobium in Superalloys", Proceedings of the International Symposium: Niobium, H. Stuart, ed., (AIME Warrendale, Pa., 1984), 1169-1219.
23. R. Decker and C. Bieber, ASTM STP No. 262, (ASTM, Philadelphia, Pa., 1959), 120-128.

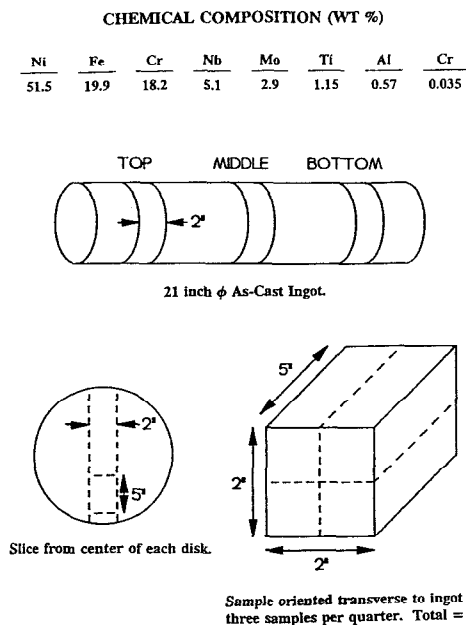


Figure 1. Chemical composition (wt%) of Alloy 718 and schematic diagram of 21" diameter ingot and location of samples used in this study.

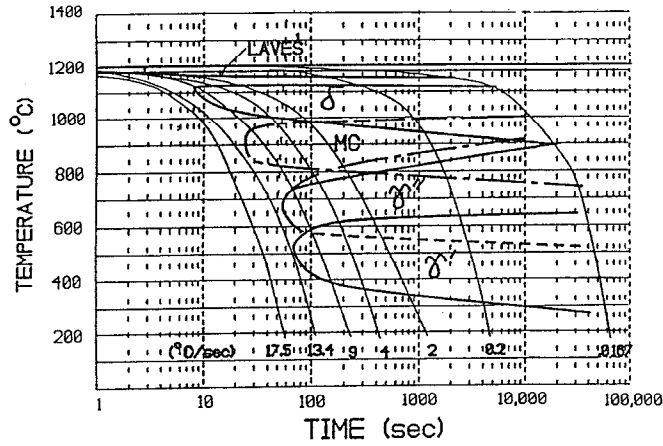


Figure 2. Continuous-Cooling-Transformation diagram of Alloy 718. Homogenized at 1180°C for 24 hours.

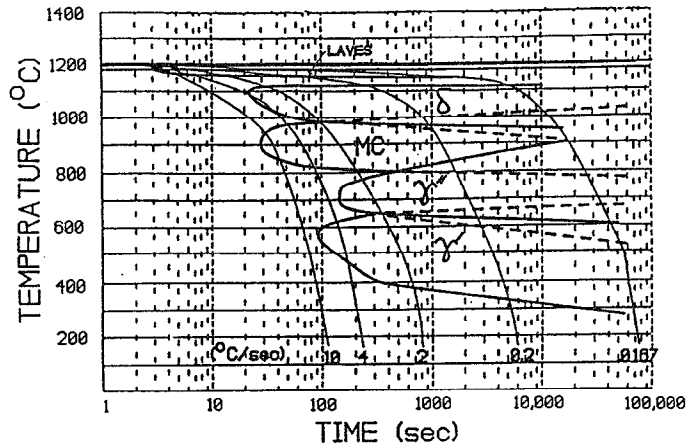


Figure 3. Continuous-Cooling-Transformation diagram of Alloy 718. Homogenized at 1180°C for 72 hours.

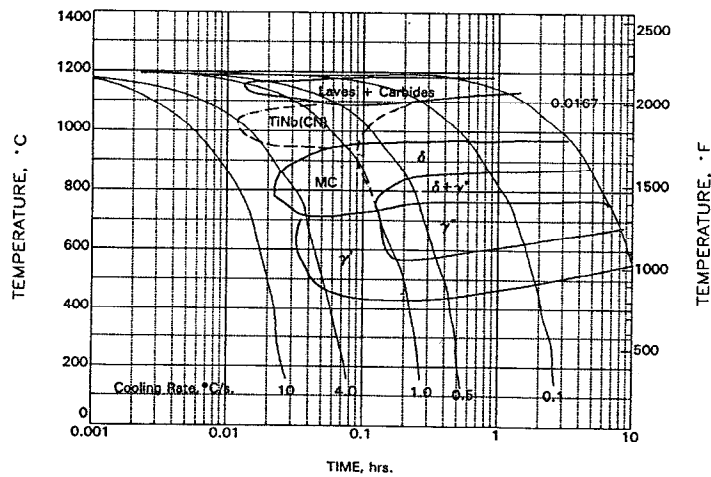


Figure 4. Continuous-Cooling-Transformation diagram of Alloy 718. Homogenized at 1180°C for 90 hours.

RECRYSTALLIZATION-TEMPERATURE-TIME MAP ALLOY 718

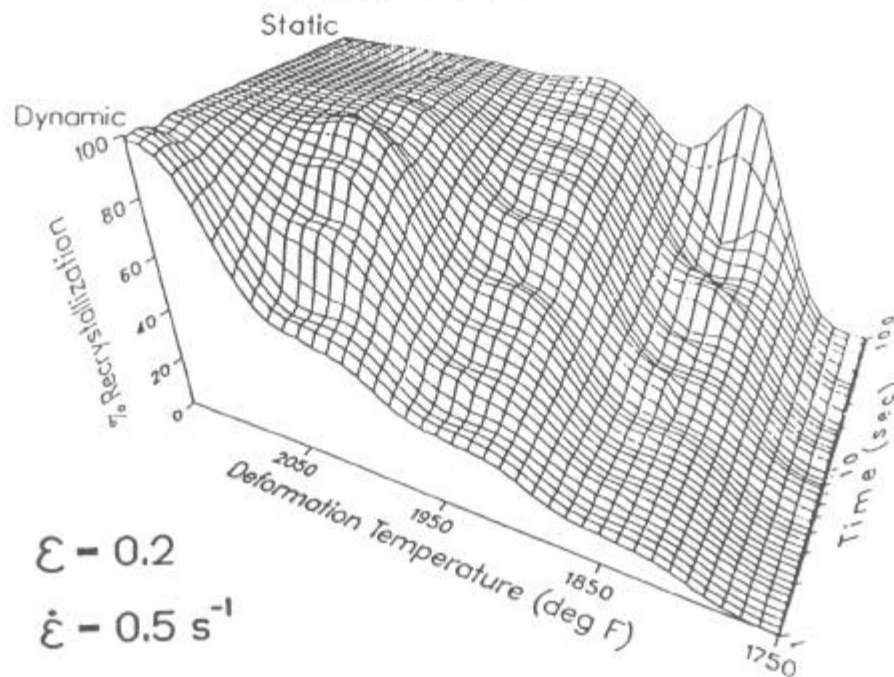


Figure 5. Recrystallization-Temperature-Time surface map for Alloy 718 under dynamic and static conditions.

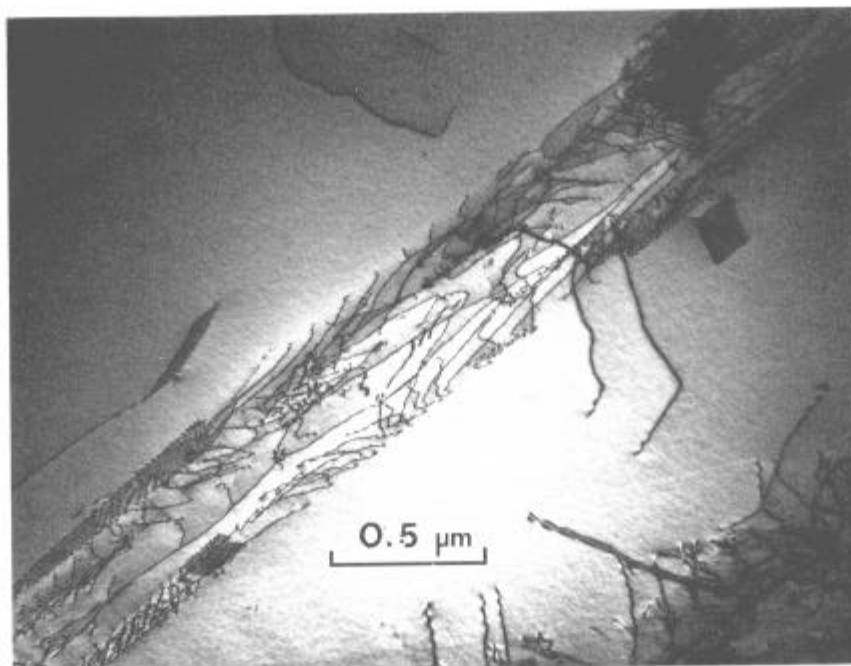


Figure 6. Dislocation structure in Alloy 718 cooled at 17° C/sec. Thin foil - TEM

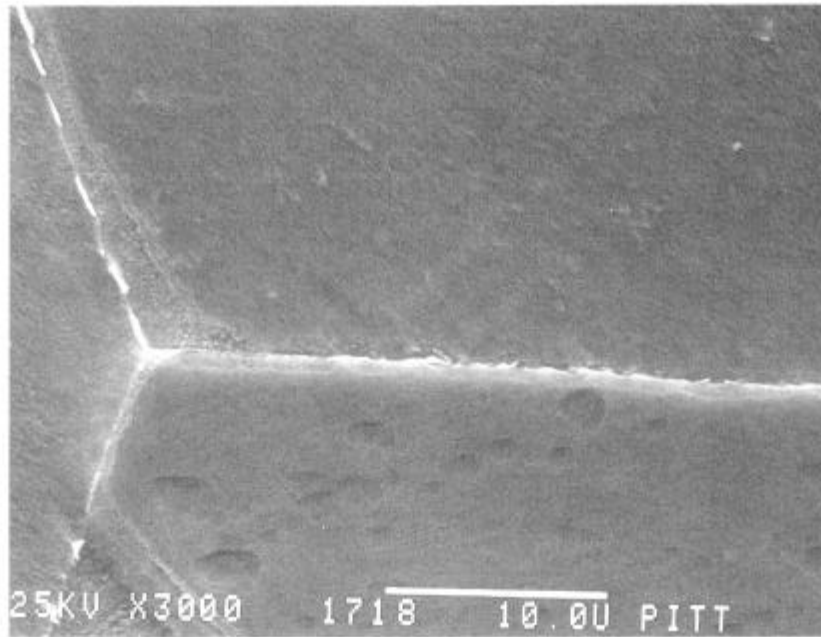


Figure 7. Precipitation of five δ particles at primary austenite grain boundaries. Alloy 718 cooled at 4°C/sec. SEM

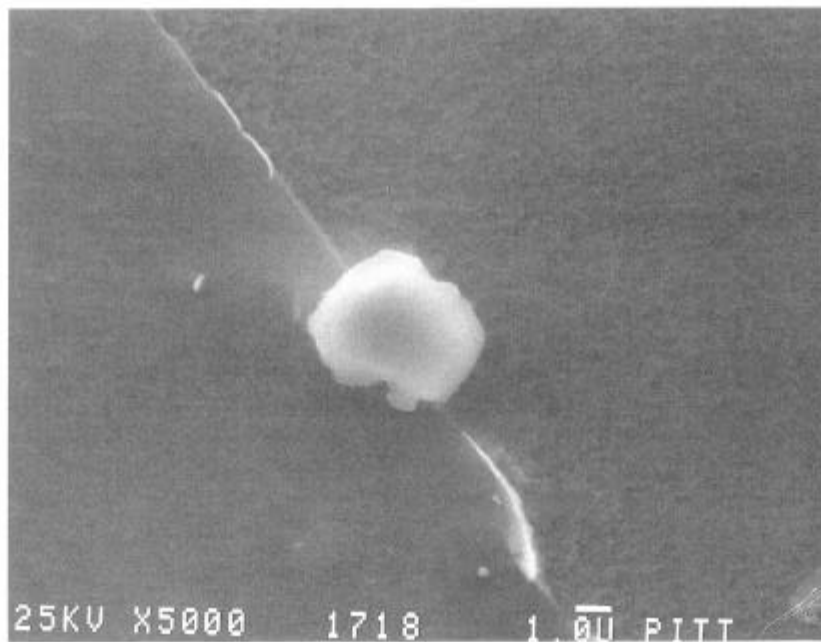


Figure 8a. Primary and new precipitated MC carbides in Alloy 718 cooled at 4°C/sec.

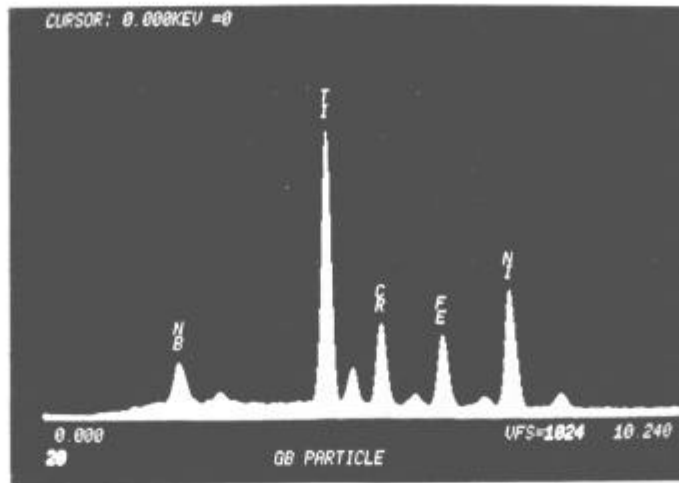


Figure 8b. X-Ray spectrum for large Ti-rich particle.

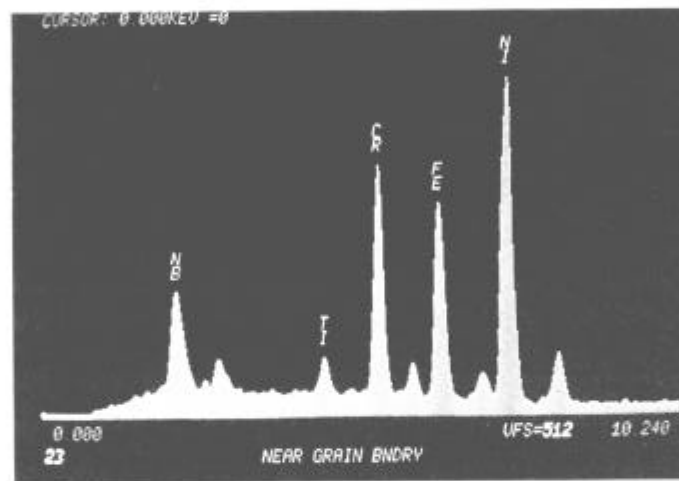


Figure 8c. X-Ray spectrum for small Nb-rich particle

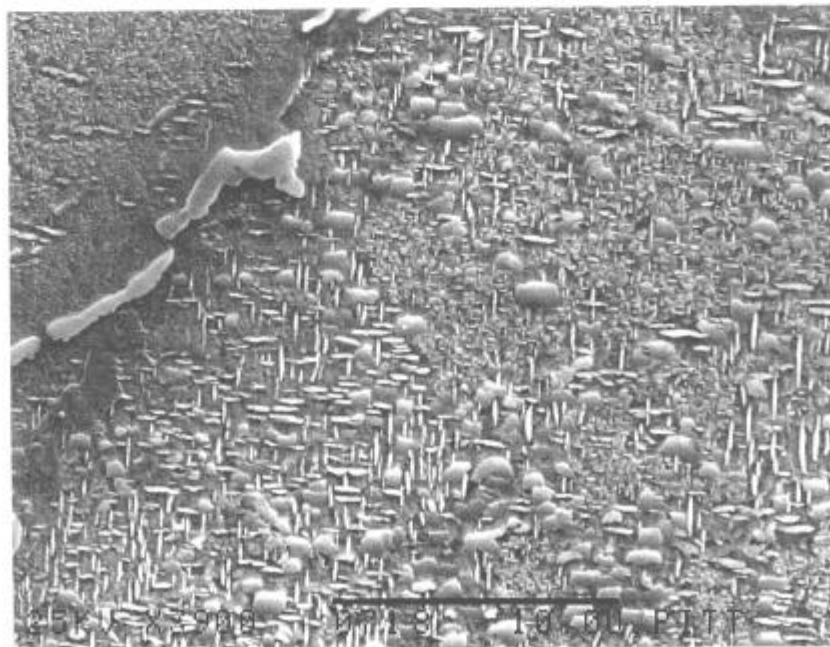
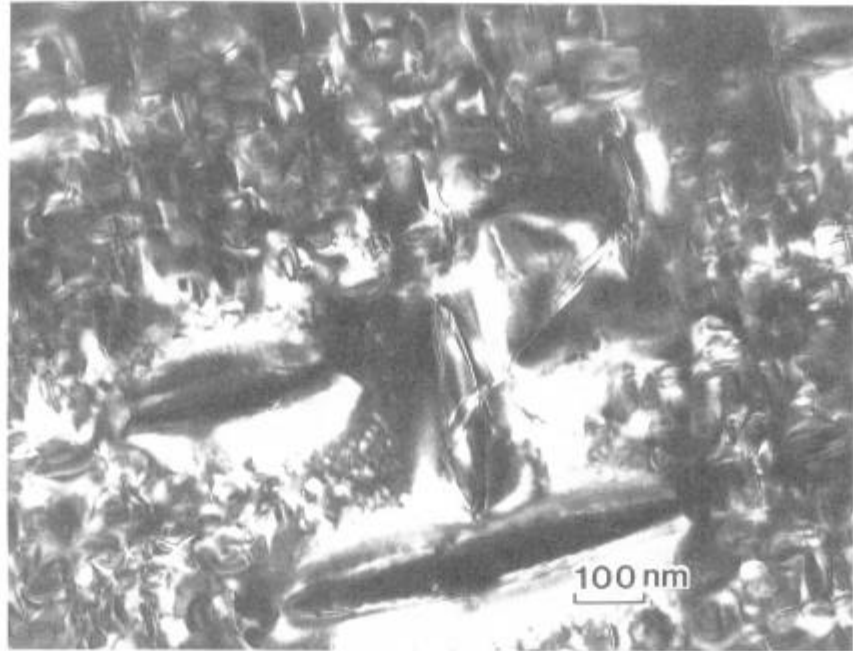


Figure 9. Typical microstructure of Alloy 718 cooled at $.0167^{\circ}\text{C}/\text{sec}$.



a. Bright field

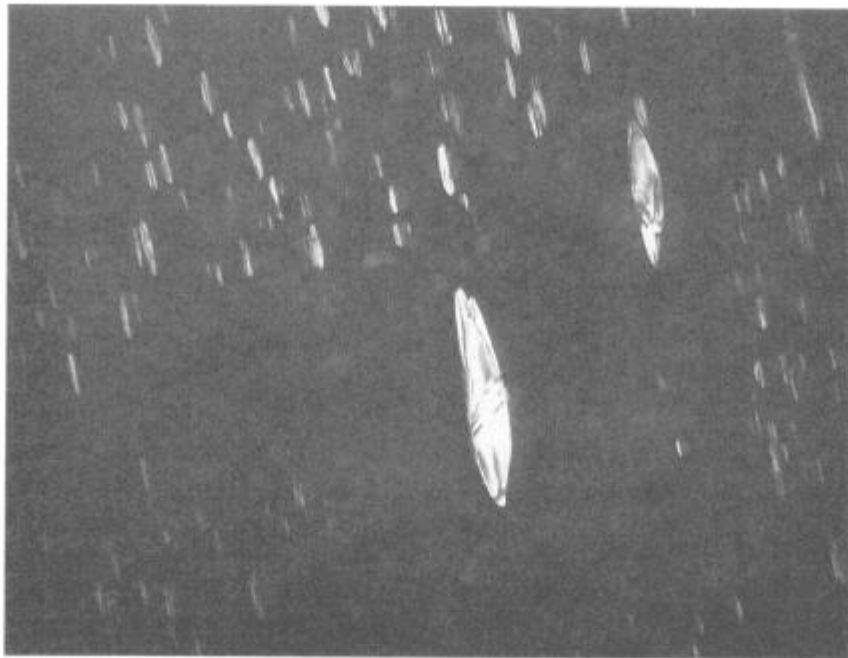


Figure 10. a,b The γ' , γ'' , and δ precipitates observed in the matrix of Alloy 718 cooled at .0167 °C/sec. Thin foil - TEM.